Tuning the Photophysical and Electrochemical Properties of Aza-Boron-Dipyridylmethenes for Fluorescent Blue OLEDs

Abegail C. Tadle, Karim A. El Roz, Chan Ho Soh, Daniel Sylvinson Muthiah Ravinson, Peter I. Djurovich, Stephen R. Forrest, and Mark E. Thompson*

A series of substituted aza-boron-dipyridylmethene (aD) compounds are demonstrated as fluorescent dopant emitters in blue organic light emitting diodes (OLEDs). Replacing the *meso*-carbon of a dipyridylmethene dye with nitrogen to form the aD chromophore leads to a destabilization of the highest occupied molecular orbital in aD, as evidenced both from their experimentally determined photophysical and electrochemical properties. These properties are consistent with theoretical calculations of the molecular energetics. These aD derivatives emit violet to blue light, peaking between 400 and 460 nm with photoluminescent quantum yields over 85%. The aD compounds have small energy differences (<400 meV) between their singlet and triplet excited states. OLEDs fabricated with an aza-boron-dipyridylmethene emitting fluorophore give an external quantum efficiency of 4.5% on glass substrates, close to the theoretical maximum for fluorescent OLEDs.

1. Introduction

Organic light emitting diodes (OLEDs) have been commercialized for use in the displays of mobile phones, tablets, televisions, and wearable technologies, as well as in solid-state lighting panels. The electroluminescent process involves

A. C. Tadle, Dr. K. A. El Roz, D. Sylvinson Muthiah Ravinson,
Prof. P. I. Djurovich, Prof. M. E. Thompson
Department of Chemistry
University of Southern California
Los Angeles, CA 90089, USA
E-mail: met@usc.edu
C. H. Soh, Prof. S. R. Forrest
Department of Physics
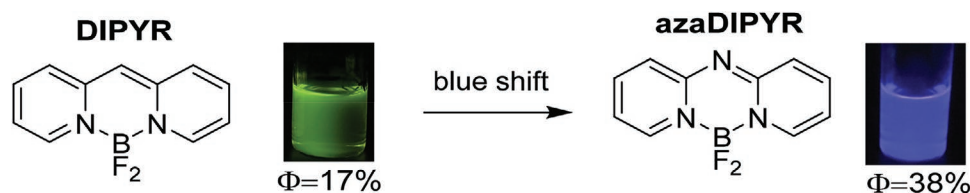University of Michigan
Ann Arbor, MI 48109, USA
Prof. S. R. Forrest
Department of Electrical and Computer Engineering
University of Michigan
Ann Arbor, MI 48109, USA
Prof. S. R. Forrest
Department of Materials Science and Engineering
University of Michigan
Ann Arbor, MI 48109, USA
Dr. M. E. Thompson
Mork Family Department of Chemical Engineering and Materials Science
University of Southern California
Los Angeles, CA 90089, USA

hole/electron recombination that leads to a mixture of singlet and triplet excitons.[1] In the late 1990's, phosphorescent emitters were incorporated into OLEDs, making it possible to harvest both types of excitons and achieve 100% internal efficiency for conversion of electrical charges into photons. OLEDs with green and red phosphorescent emitters have been shown to achieve both high quantum efficiencies and long device lifetimes, and have thus become standard emissive dopants in commercial OLED displays.[2] While the internal quantum efficiencies of OLEDs utilizing blue phosphorescent dopants have also reached the theoretical limit of 100%, the operational lifetimes of these devices have thus far been short and needs to be improved for practical application in displays.[3] The stability of blue phosphorescent OLEDs is limited by degradation of the host and/or dopant materials via bimolecular decay processes, that is, exciton-exciton or exciton-polaron annihilation.[3],[4] These second order processes are exacerbated by the long excited state decay lifetimes of phosphorescent emitters, typically a few microseconds. Fluorescent blue emitters are less efficient in OLEDs, but their markedly shorter excited state lifetimes (nanoseconds) dramatically reduce the rate of bimolecular decay, thereby increasing the device's operational lifetime. Thus, fluorescence-based blue dopants are conventionally used for OLEDs in commercial displays.

Blue fluorescent materials also have utility in white OLEDs (WOLEDs) for solid state lighting.[5] Our interest in blue fluorophores stems from a device architecture that splits the singlet and triplet excitons spatially within the WOLED, allowing for the singlet excitons to be harvested on a blue fluorescent dopant and the triplets on red and green phosphorescent dopants.[5],[6] This hybrid fluorescent/phosphorescent WOLED has the potential to give high color quality with an internal quantum efficiency of 100%, without the need for blue phosphors. However, aside from highly efficient blue luminescence, the energy of the triplet state of the fluorescent dopant in this architecture needs to be high enough to enable endothermic energy transfer to the green-to-red phosphorescent dopant. This requirement places a restriction on the most common structural motifs used to create fluorescent blue lumiphores (stilbenes, anthracenes, etc.), as energies for the triplet state in these materials are typically too low ($E_T < 2$ eV) for effective energy transfer to the phosphor. Therefore, the hybrid WOLED puts a constraint on

Figure 1. Atomic transmutation of meso-position in DIPYR from methine-bridge to imine-bridge alters the optical properties of the molecule. Photoluminescence quantum yields were obtained in methylcyclohexane.

the fluorophore in that it needs to have a blue emissive singlet and a high triplet energy, thus requiring a small energy difference between the singlet and triplet excited states (ΔE_{ST}), preferably with $\Delta E_{ST} < 400$ meV.

Here, we focus on a **DIPYR** (boron dipyridylmethene, **Figure 1**) family of dyes[7] to achieve highly efficient blue fluorescence in OLEDs. **DIPYR** dyes are related to the more widely studied BODIPY (4,4-difluoro-4-bora-3a,4a-diaza-s-indacene) chromophores, dyes that have high photoluminescent efficiencies ($\Phi_{PL} > 0.8$), short emission lifetimes ($\tau < 10$ ns), and narrow emission linewidths (full width half maxima, fwhm < 50 nm). However, shifting the emission color of BODIPY into the blue is difficult, and these compounds have intrinsically low triplet energies.[8] These drawbacks make **DIPYR** motifs attractive alternatives for blue fluorescent dopants for use in WOLEDs.

A simple transmutation from methene to imine converts the green-emissive **DIPYR** to a blue emissive **azaDIPYR (aD)** (Figure 1). This structural modification stabilizes the energy of the highest occupied molecular orbital (HOMO), but leaves the lowest unoccupied molecular orbital (LUMO) relatively unperturbed, thereby inducing a hypsochromic shift in the emission energy.[9] The emission lifetimes of $\tau < 10$ ns of **DIPYRs** are suitable for use in OLEDs, but the low Φ_{PL} limits the external quantum efficiency (EQE). Previous work on **DIPYR** compounds suggests that benzannulation of the molecular core can improve photoluminescence efficiency while maintaining the short emission lifetime and narrow linewidths.[9b,10] We have examined benzannulation along with substitution around the core structure to modify the photophysical properties of a set of **aD** molecules shown in **Figure 2**. Heterocyclic ligands conjugated with boron fluoride, analogous to the **aD** core, have been previously investigated as dyes,[9a,11] aggregation-induced emitters,[12] and pH sensors,[13] but few studies have been reported on **aD** materials as emitters aside from a citation in the patent literature.[14] Benzannulated derivatives of the **aD** core are potentially useful as blue fluorescent dopants due to their narrow

emission profile, nanosecond lifetime, high thermal stability, and high Φ_{PL}. The development of these organic blue-emitting materials is described, including their synthesis, electrochemical and photophysical characterization, and performance of **2a** in blue OLEDs.

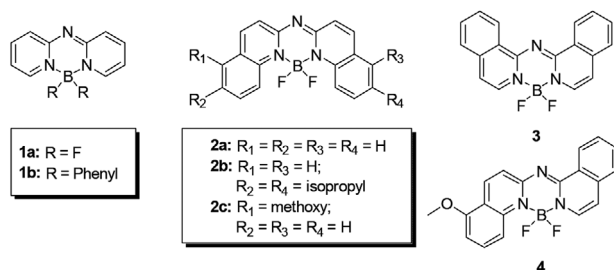## 2. Results and Discussion

2.1. Synthesis

The synthesis of the **aD** dyes follows a procedure similar to one previously reported (**Figure 3**).[9a,13a] A palladium catalyzed coupling reaction of 2-amino and 2-bromo substituted heteroaryl compounds were used to form the desired ligand. The ligand was deprotonated with Hunig's base and treated with $BF_3 \cdot OEt_2$ to give the **aD** dye. The aryl substituted derivative was prepared by treating the ligand with 2-aminoethoxydiphenyl borate. The products were obtained as microcrystalline solids, which are white-to-yellow for **1a-1b** and bright yellow for **2a-c**, **3**, and **4**.
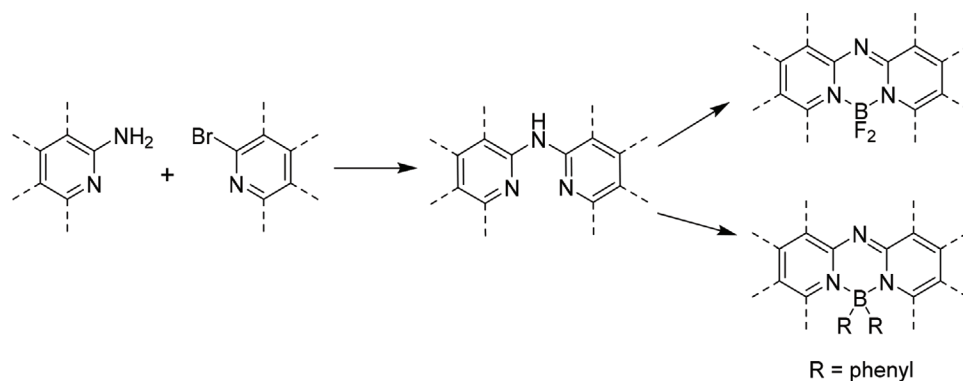
2.2. Electrochemistry

The electrochemical properties of the **aD** compounds were analyzed by cyclic voltammetry (CV), see **Table 1**. Oxidation is irreversible for all the compounds, whereas reduction is irreversible for **1a-1b** and reversible or quasi-reversible in the benzannulated derivatives, that is, **2a-2c**, **3**, **4**. The oxidation potentials of the **aD** dyes span a range of 0.72–1.15 V ($\Delta E_{redox} \approx 400$ meV). The reduction potentials span a larger range of –1.91 to –2.59 V ($\Delta E_{redox} \approx 700$ meV). The potentials of the benzannulated derivatives **2a-2c**, **3**, **4** are anodically shifted relative to **1a-1b**, suggesting stabilization of both the filled and vacant frontier molecular orbitals, similar to what is observed in the DIPYR system.[9b] Addition of substituents such as isopropyl (**2b**) or methoxy (**2c** and **4**) groups leads to the cathodic shifts in both oxidation and reduction potentials. For example, the electrochemical potentials of **2c** are shifted relative to **2a** by 0.21 V for oxidation and 0.12 V for reduction.

2.3. Photophysical Characterization

The UV-visible absorption spectra of **1a-1b**, **2a-2c**, **3**, and **4** are shown in **Figure 4**. All of the **aD** compounds have high molar absorptivities ($\varepsilon \approx 10^4$–10^5 M^{-1} cm^{-1}), similar to dyes such as fluorescein, BODIPY, and porphyrin. The **aD** compounds display vibronically structured π-π^* absorption bands between 300 and

Figure 2. Structures of aza-boron-dipyridylmethene (aD) in this work.

**ADVANCED
SCIENCE NEWS**

www.advancedsciencenews.com

**ADVANCED
FUNCTIONAL
MATERIALS**

www.afm-journal.de

Figure 3. General synthetic scheme to make substituted aza-boron-dipyridylmethene derivatives. Precursors can be pyridyl, quinolyl, or isoquinolyl. Detailed procedures are given in the Supporting Information.

445 nm. The lowest energy absorption bands in compounds **1a-1b** (λ_{max} = 395–410 nm) are broader than the same transitions in **2a-2c**, **3**, and **4** (λ_{max} = 420–445 nm). The decrease in absorption energy in the benzannulated derivatives follows a related decrease in the redox gap, Table 1. The full width half maximum for the 0-0 transition is narrow in **2a-2c** (fwhm = 310 cm^{-1}) and **3**, **4** (fwhm = 515 cm^{-1}). Narrow linewidths are similarly observed for the structurally related DIPYR dyes.[9b] The intensity ratios for the 0-0 to 0-1 transitions in **1a-1b** are also smaller than in the benzannulated derivatives. The narrow linewidths along with the large ratio in 0-0 to 0-1 transition intensity suggest that the benzannulated compounds undergo minimal structural change in their excited states.

Photoluminescence spectra of **1a-1b**, **2a-2c**, **3**, and **4** are shown in **Figure 5** and their photophysical data are summarized in **Table 2**. The photophysical properties of poly(methyl methacrylate) (PMMA) films doped at 1% with the **aD** dyes are similar to those in solution (see Supporting Information). The **aD** series give fluorescent emission between λ_{em} = 400–450 nm. Compounds **1a-1b** exhibit violet-to-blue fluorescence spectra that are mirror images of their absorption bands. The Stokes shift increases from 6 nm for **1a** to 20 nm upon addition of phenyl groups in **1b**. The emission profiles of the benzannulated derivatives are bathochromically shifted compared to the non-benzannulated analogs, yet they retain similar vibrational features with an average Stokes shift of ≈4 nm. Phosphorescence spectra for **aD** compounds taken in 2-MeTHF at 77 K have emission maxima ≈460 nm for **1a-1b** and 484–502 nm

for **2a-2c**, **3**, and **4** (Figure 5). The E_{0-0} energies for the lowest excited singlet (S$_1$) and triplet (T$_1$) states determined from the peak maxima of the fluorescence and phosphorescence emission spectra, respectively, are given in Table 2. The compounds have a cyanine-like property where there is relatively little orbital overlap between the HOMO and LUMO as these orbitals are distributed on different atoms in the molecule. Thus, Franck–Condon factors are correspondingly small, minimizing vibronic coupling and structural relaxation in the excited state leading to a narrow emission line shape.[15] In addition, this orbital configuration gives rise to the small energy for the singlet-triplet gap of these materials.

The photoluminescence quantum yields of the benzannulated compounds in solution and in doped PMMA film are high (Φ_{PL} > 0.80). Polymer films doped at high concentrations (>1 wt%) display bathochromic shifts, broadened emission spectra, and lower quantum yields due to self-absorption, as expected for fluorophores with small Stokes shifts.[16] The excited state lifetimes (τ = 2 to 4 ns) and radiative rates [k_r = (0.93–3.2) x 10^8 s^{-1}] are similar across the series, which aligns with common organic fluorophores.[17] However, the non-radiative rates are an order of magnitude higher for the non-benzannulated compounds (k_{nr} = 10^8 s^{-1}) relative to the benzannulated derivatives (k_{nr} = 10^7 s^{-1}). The higher non-radiative rates in the non-benzannulated derivatives are attributed to the faster rates for intersystem crossing (ISC) in these systems.[9b]

The singlet and triplet excited state energies were calculated using TD-DFT (B3LYP functional, 6-311G** basis set; see Supporting Information for details). Previous studies with BF$_2$-pyridylmethene and BODIPY dyes have shown that these DFT tends to overestimate the singlet energy but give acceptable values for the triplets.[8l,9b,18] Thus, a correction factor of −0.44 eV is needed for the calculated singlet energies to align with the experimental values. The corrected S$_1$ and uncorrected T$_1$ state energies predicted by these modeling studies fall within 0.2 eV of spectroscopically determined values. Intersystem crossing transitions between the S$_1$ and T$_1$ states are symmetry forbidden, hence a comparatively slow rate for ISC is expected for S$_1$→T$_1$. However, the S$_1$→T$_2$ transition is symmetry allowed, so it is important for the T$_2$ state to be higher in energy than the S$_1$ state to prevent ISC via S$_1$→T$_2$ from being competitive with fluorescence. The T$_2$ state is lower in energy than S$_1$ in

Table 1. Electrochemical potentials of **1a-1c**, **2a-2c**, **3** and **4**.

|	E_{ox} [V][a]	E_{red} [V][a]	ΔE_{redox} [V]
1a	+0.92	−2.30	3.22
1b	+0.72	−2.59	3.31
2a	+1.15	−1.91	3.06
2b	+1.08	−1.98	3.06
2c	+1.09	−2.07	3.16
3	+1.10	−2.09	3.19
4	+1.04	−2.14	3.18

[a] Redox potentials obtained from cyclicvoltammetry in acetonitrile with ferrocenium/ferrocene as an internal standard.
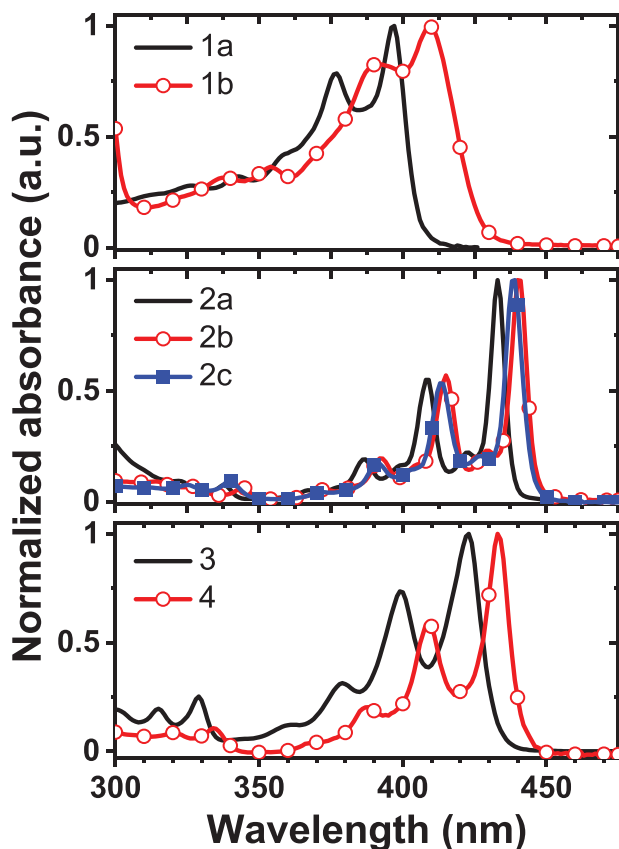
Figure 4. Normalized absorption spectra for **aD** dyes in 2-MeTHF at 298 K. The full width half maximum (fwhm) for the 0-0 transition is narrow in **2a-2c**.

1a-1b, but is calculated to be higher than S_1 in **2a-2c**, **3**, and **4**. Thus, low quantum yields ($\Phi_{PL} \leq 42\%$) for derivatives **1a-1b** are attributed to exergonic ISC between the S_1 and T_2 states.[9b] Benzannulation in **aD** dyes stabilizes the S_1 state more than the T_2 state, thereby making the $S_1{\rightarrow}T_2$ transition thermodynamically unfavorable.

The experimental S_1-T_1 gaps fall in a small range within the **aD** series (ΔE_{ST} = 0.20–0.45 eV). The largest gap is observed for **1a** (ΔE_{ST} = 0.44 eV), where the singlet and triplet gap is similar to that of **DIPYR** (ΔE_{ST} = 0.42 eV) and the benzannulated **DIPYR** derivatives (ΔE_{ST} = 0.43–0.48 eV).[9b] Interestingly, the **aD** benzannulated derivatives have singlet-triplet gaps smaller than the parent **aD** compound (**1a**). Quinoline-based systems (**2a-2c**) maintain a $\Delta E_{ST} \approx 0.30$ eV, whereas isoquinoline systems (**3** and **4**) have a larger gap ($\Delta E_{ST} \approx 0.40$). To determine the origin of the small S_1-T_1 gaps in the **aD** compounds, the extent of spatial overlap (Λ) between the hole and electron natural transition orbitals (NTOs) was calculated for transitions associated with the first excited states (S_1/T_1) (see Supporting Information for details). The value of Λ is near unity for strongly localized excitations such as in π-π^* transitions (where the hole and electron involve the same orbitals), giving rise to a large ΔE_{ST}, and Λ close to 0 for purely CT transitions with little or no spatial overlap, and thus a small ΔE_{ST}. The computed Λ values and experimental S_1-T_1 gaps of the **aD** series are intermediate between those of a localized transition (anthracene)[19] and a nearly pure CT state (4CzIPN).[20] Both S_1 and T_1 states in the **aD** compounds show similar degrees of spatial overlap (**1a-1b**, Λ = 0.64 and 0.68, respectively; **2a-2c**, **3** and **4**, Λ = 0.61–0.68). Λ is 0.84 for anthracene (ΔE_{ST} = 1.46 eV) and 0.29 for 4CzIPN (ΔE_{ST} = 0.10 eV). It is evident that the small Λ range, with $\approx$0.15 difference between the highest and lowest value, is responsible for the relatively invariant $\Delta E_{ST} \approx 0.30$ eV found in the benzannulated derivatives.
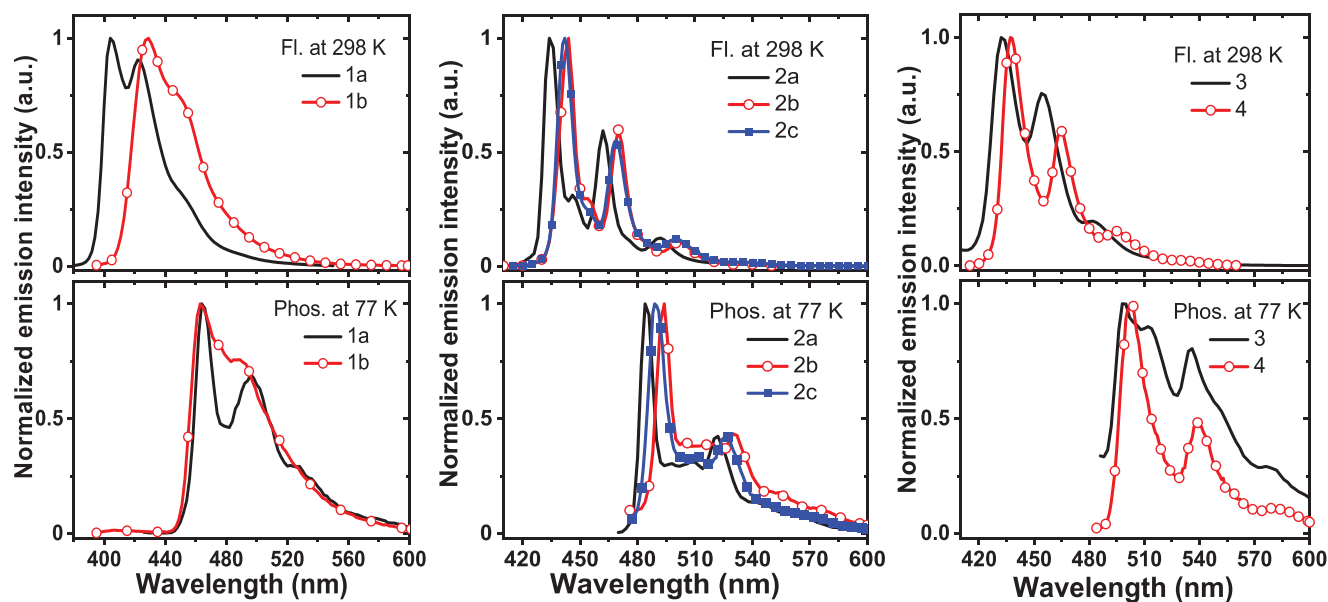
Figure 5. Normalized emission spectra at room temperature (upper plots), and gated phosphorescence emission (bottom plots) recorded after 500 µs delay time at 77 K. Measurements were performed in 2-methyltetrahydrofuran (2-MeTHF).

Table 2. Summary of the photophysical parameters for **1a-1b**, **2a-2c**, **3**, and **4**.

	λ_{abs} [nm][a]	$\lambda_{em\ max}$ [nm][b]	Φ_{PL}	τ [ns]	k_r [10^8 s^{-1}][c]	k_{nr} [10^8 s^{-1}][d]	$\lambda_{em\ max}$ [nm][e]	ΔE_{ST} [eV]
1a	398	404	0.42	2.1	2.0	2.7	464	0.44
1b	409	429	0.30	2.1	1.4	3.4	463	0.34
2a	433	434	0.86	3.3	2.7	0.43	484	0.30
2b	440	444	0.87	3.8	2.3	0.34	494	0.30
2c	441	442	0.84	3.3	2.6	0.49	488	0.27
3	422	432	0.87	3.2	2.8	0.41	498	0.44
4	433	437	0.90	2.8	3.2	0.36	502	0.39

[a] Recorded in 2-MeTHF; [b] Fluorescence measured at 298 K; [c] $k_r = \Phi_{PL}/\tau$; [d] $k_{nr} = (1-\Phi_{PL})/\tau$; [e] Phosphorescence measured at 77 K.

2.4. Electroluminescence

OLEDs were fabricated using compound **2a** as an emissive dopant since its frontier orbital energies and photophysical properties are representative of the **aD** series. The photoluminescence properties of **2a** are also not significantly affected by solvent polarity (see Supporting Information), suggesting that a wide range of host materials with different dielectric constants can be employed to equal effect. Compounds reported to be effective hosts for fluorescent blue dopants in OLEDs, N,N'-di(1-naphthyl)-N,N'-diphenyl-(1,1'-biphenyl)-4,4'-diamine (NPD),[21] bis[2-(diphenylphosphino)phenyl] ether oxide (DPEPO),[22] 2,6-bis(3-(carbazol-9-yl)phenyl)pyridine (26DCzPPy)[23] and 4,4'-bis(N-carbazolyl)-1,1'-biphenyl (CBP)[24] were investigated as host materials for **2a**. NPD and DPEPO proved to be poor host materials; NPD films doped at 1 and 10 wt% percent **2a** exhibit a broad photoluminescence between 470 and 750 nm, whereas OLEDs with an emissive layer (EML) of **2a** doped in DPEPO displayed featureless electroluminescence between 550 and 750 nm, which is attributed to emission from an exciplex (see Supporting Information). Fortunately, photoluminescence spectra of **2a** doped at 1 and 5 wt% in CBP and 26DCzPPy hosts retain the sharp vibronic emission bands observed in solution. However, the small Stokes shift of **2a** leads to the reabsorption of emitted photons resulting in self-quenching of the fluorophore when doped at high concentrations. The intensity of the (0-0) photoluminescent emission peak of **2a** (λ_{max} = 453 nm), decreases markedly in 5 wt% films (**Figure 6**). The PL efficiency of CBP and

26DCzPPy films doped at 1 wt% were higher (Φ_{PL} = 0.71 and 0.66, respectively) than those doped at 5 wt% (Φ_{PL} = 0.39 and 0.43, respectively). OLEDs with a 15 nm thick EML were fabricated with **2a** doped at 1 wt% into CBP or 26DCzPPy. The hole transport layer consisted of 10 nm of dipyrazino[2,3,-f:20,30-h]quinoxaline 2,3,6,7,10,11-hexacarbonitrile (HATCN) and 45 nm of 4,4'-cyclohexylidenebis[N,N-bis(4-methylphenyl)benzenamine] (TAPC), whereas the electron transport layer comprised of 45 nm of 4,7-diphenyl-1,10-phenanthroline (Bphen) and 1.5 nm of (8-quinolinolato)lithium (LiQ) (1.5 nm). Indium tin oxide (ITO) was used as the anode and aluminum as the cathode. The properties of the OLEDs are tabulated in **Table 3**.

Figure 7 shows the device architecture (Figure 7A) employing CBP.[25] The electroluminescent emission spectrum in Figure 7B retains the sharp and narrow vibronic structure with increasing current density (J = 1–100 mA cm^{-2}); similar EL spectra are observed in devices using 26DCzPPy (see Supporting Information). The turn-on voltage of CBP (V_{on} = 3.5 V; Figure 7C and Table 3) is lower than 26DCzPPy (V_{on} = 4.5 V). Additionally, the maximum EQE for CBP (4.5 ± 0.2%) is higher than 26DCzPPy (3.5 ± 0.2%) and closer to the theoretical maximum of ≈5% in a fluorescent OLED on a glass substrate (Figure 7D). One drawback in these devices is the steep roll-off in EQE at high current densities, likely caused by hole leakage since the HOMO energy in **2a** (−6.11 eV) is lower than that of either host (CBP, −5.80 eV; 26DCzPPy, 6.05 eV). The small peak observed between wavelengths of 380 and 410 nm with increasing current is attributed to emission from Bphen owing to the hole leakage in these devices (see Supporting
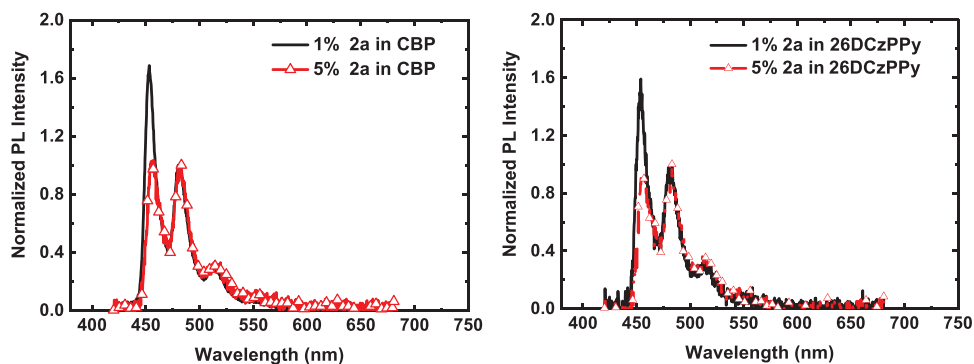
Figure 6. PL emission of 1% and 5% **2a** dopant in CBP and 26DCzPPY host materials.

Table 3. Properties of OLEDs doped with 1 wt% **2a** into CBP and 26DCzPPy hosts.

Host	λ_{max} EL [nm]	V_{on} [V]	EQE_{max} [%]	EQE [%, 100 cd m^{-2}]	EQE [%, 1000 cd m^{-2}]	CIE coordinate
CBP	445	3.0	4.5[a]	4.1	2.7	(0.15, 0.14)
26DCzPPy	445	3.7	3.5	3.5	2.7	(0.15, 0.14)

[a]Maximum EQE is the average of 7 devices with a standard deviation of 0.13.

Information). The observed high EQE of **2a** in CBP could be due to one of two scenarios: one where the device architecture is optimized and the dopants are isotopically aligned or one where the dopants have significant horizontal alignment but the device architecture has not been completely optimized. Based on the hole leakage observed in these devices, the latter seems more likely. Further studies are needed to determine the molecular orientation of these blue dopants.

3. Conclusion

Substituted aza-boron-dipyridylmethenes (**aD**) were explored as candidates for fluorescent blue dopants in OLEDs. The synthetic flexibility of these materials makes them easy to modify with different substituents to alter their energetics, while also maintaining the high quantum efficiency, small S_1-T_1 gap, and small Stokes shift. Seven substituted **aD** compounds were synthesized to study their photophysical and electrochemical properties. All of the benzanullated compounds display blue fluorescence ($\lambda_{em} = 400$–500 nm) with quantum efficiencies >85%. Minimal overlap between the HOMO and LUMO leads to the small singlet-triplet energy gaps of these materials

($\Delta E_{ST} \leq 0.4$ eV). OLEDs prepared using one of these derivatives (**2a**) have low turn-on voltages (3 V) and high efficiency ($EQE_{max} = 4.5 \pm 0.2\%$), approaching the maximum theoretical limit of fluorescent OLEDs on glass substrates (EQE = 5%). These studies suggest that **2a** and the other compounds in the **aD** series can serve as fluorescent blue dopants in both monochromatic and WOLEDs. Furthermore, their small single-triplet energy gaps present an opportunity to harvest the triplet excitons to increase the internal quantum efficiency in hybrid fluorescent/phosphorescent white light emitting diodes.

4. Experimental Section

Synthesis: Precursors for **1a-1b** were purchased from Sigma Aldrich. Aza-boron-dipyridylmethene (aD) synthesis for **1a-1b, 2a-2c, 3,** and **4** were prepared using similar coupling reaction synthesis with pyridine, quinoline, or isoquinoline core.[13b] The detailed synthesis and characterization of each of the compounds are given in the Supporting Information.

Electrochemical Measurements: Cyclic voltammetry and differential pulsed voltammetry were performed using a VersaSTAT potentiostat measured at 100 mV s^{-1} scan. Anhydrous acetonitrile (DriSolv) from Sigma Aldrich was used as the solvent under nitrogen environment, and 0.1 M tetra(n-butyl)ammoniumhexafluorophosphate was used as
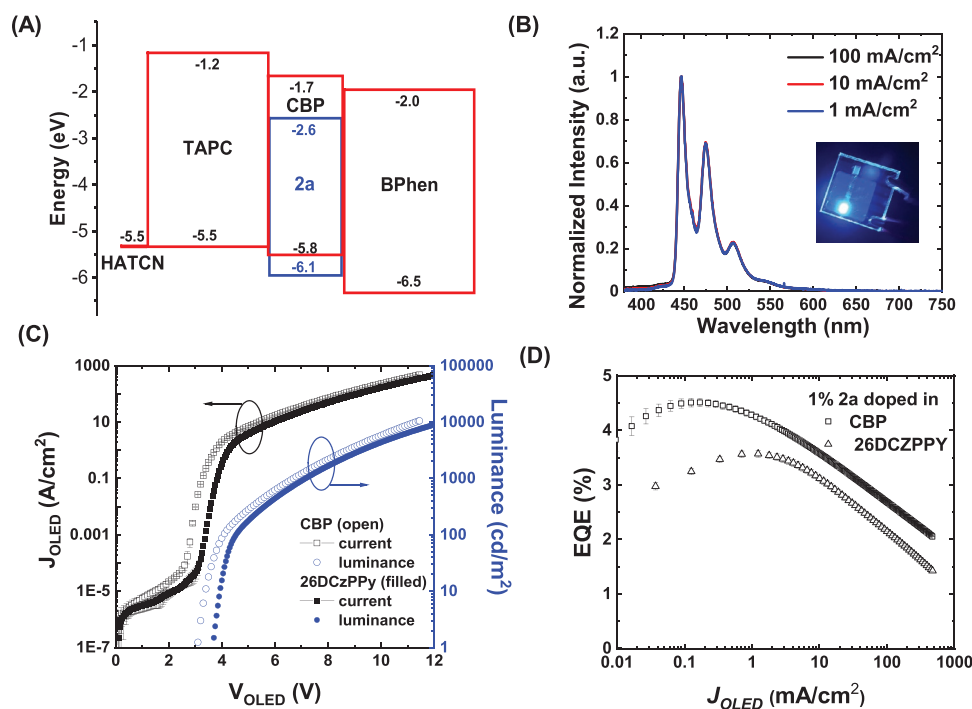
Figure 7. A) Device architecture and energy levels of an OLED with CBP host and **2a** dopant. B) Electroluminescence spectra with increasing current (1–100 mA cm^{-2}). C) Current versus voltage plots and D) EQE versus current plots for devices using CBP and 26DCzPPy hosts.

the supporting electrolyte. A glassy carbon rod was used as the working electrode; a platinum wire was used as the counter electrode, and a silver wire was used as a pseudoreference electrode. The redox potentials were based on values measured from differential pulsed voltammetry and were reported relative to a ferrocenium/ferrocene (Cp_2Fe^+/Cp_2Fe) redox couple used as an internal reference; electrochemical reversibility was determined using cyclic voltammetry.

Photophysical Measurements: All samples in fluid solution were dissolved in 2-methyltetrahydrofuran (2-MeTHF) with absorbance between 0.05 and 0.15 to prevent reabsorption when performing photoluminescence measurements due to the small Stokes shift in the aD series. Doped PMMA thin films were prepared from a solution of PMMA in dichloromethane. Samples of **1a**, **2a**, and **3** (1 vol%) were dissolved in the PMMA solution and spin coated on a quartz substrate (2 cm x 2 cm) rotating at 700 rpm for 45 s. The UV-visible spectra were recorded on a Hewlett–Packard 4853 diode array spectrometer. Steady state fluorescence emission measurements were performed using a QuantaMaster Photon Technology International spectrofluorometer. Gated phosphorescence measurements were carried on the fluorimeter using a 500 microsecond delay on samples at 77 K. All reported spectra were corrected for photomultiplier response. Fluorescence lifetime measurements were performed using an IBH Fluorocube instrument equipped with 331 nm LED and 405 nm laser excitation sources using a time-correlated single photon counting method. Photoluminescence quantum yields were obtained using the C9920 Hamamatsu integrating sphere system.

Molecular Modeling: All calculations reported in this work were performed using the Q-Chem 5.1 program. Ground-state optimization calculations were performed using B3LYP functional along with 6-311G** basis set. Time dependent density functional theory calculations on the ground-state optimized geometries were performed using B3LYP/6-311G** level. The singlet energies were corrected by subtracting 0.44 eV as a correction factor commonly used for cyanine-like dyes.[9b]

Device Fabrication: OLEDs were fabricated and tested on glass substrates with pre-patterned, 1 mm wide ITO stripes cleaned by sequential sonication in tergitol, deionized water, acetone, and isopropanol, followed by 15 min UV ozone exposure. Organic materials and metals were deposited at rates of 0.5–2 Å s^{-1} through shadow masks in a vacuum thermal evaporator with a base pressure of 10^{-7} Torr. A separate shadow mask was used to deposit 1 mm wide stripes of 100 nm thick Al films perpendicular to the ITO stripes to form the cathode, resulting in a 1 mm[2] device area. The device structure was: glass substrate/70 nm ITO/10 nm dipyrazino[2,3,-f:20,30-h]quinoxaline 2,3,6,7,10,11-hexacarbonitrile (HATCN)/45 nm 4,4′-cyclohexylidenebis[N,N-bis(4-methylphenyl)benzenamine] (TAPC)/1 wt% **2a**: 4,4′-bis(N-carbazolyl)-1,1′-biphenyl (CBP) host/45 nm 4,7-diphenyl-1,10-phenanthroline (BPhen)/1.5 nm (8-quinolinolato)lithium (LiQ)/100 nm Al. A semiconductor parameter analyzer (HP4156A) and a calibrated large area photodiode that collected all light exiting the glass substrate in the viewing direction were used to measure the J–V–luminance characteristics. The device spectra were measured using a fiber-coupled spectrometer.

Supporting Information

Supporting Information is available from the Wiley Online Library or from the author.

Acknowledgements

Conflict of Interest

The authors declare no conflict of interest.

Data Availability Statement

Research data are not shared.

[1] a) H. Yersin, in *Transition Metal and Rare Earth Compounds: Excited States, Transitions, Interactions III*, Springer, Berlin **2004**, pp. 1-26; b) M. Pfeiffer, S. R. Forrest, K. Leo, M. E. Thompson, *Adv. Mater.* **2002**, *14*, 1633.

[2] a) C. Adachi, M. A. Baldo, S. R. Forrest, S. Lamansky, M. E. Thompson, R. C. Kwong, *Appl. Phys. Lett.* **2001**, *78*, 1622; b) M. A. Baldo, D. F. O'Brien, A. You, A. Shoustikov, S. Sibley, M. E. Thompson, S. R. Forrest, *Nature* **1998**, *395*, 151; c) J. Brooks, Y. Babayan, S. Lamansky, P. I. Djurovich, I. Tsyba, R. Bau, M. E. Thompson, *Inorg. Chem.* **2002**, *41*, 3055; d) S. Lamansky, P. Djurovich, D. Murphy, F. Abdel-Razzaq, R. Kwong, I. Tsyba, M. Bortz, B. Mui, R. Bau, M. E. Thompson, *Inorg. Chem.* **2001**, *40*, 1704; e) S. Lamansky, R. C. Kwong, M. Nugent, P. I. Djurovich, M. E. Thompson, *Org. Electron.* **2001**, *2*, 53.

[3] a) W. Shih-Wen, L. Meng-Ting, C. H. Chen, *J. Disp. Technol.* **2005**, *1*, 90; b) J. Lee, C. Jeong, T. Batagoda, C. Coburn, M. E. Thompson, S. R. Forrest, *Nat. Commun.* **2017**, *8*, 15566; c) C. Adachi, R. C. Kwong, P. Djurovich, V. Adamovich, M. A. Baldo, M. E. Thompson, S. R. Forrest, *Appl. Phys. Lett.* **2001**, *79*, 2082; d) J. Zhuang, W. Li, W. Su, Y. Liu, Q. Shen, L. Liao, M. Zhou, *Org. Electron.* **2013**, *14*, 2596; e) K. P. Klubek, S.-C. Dong, L.-S. Liao, C. W. Tang, L. J. Rothberg, *Org. Electron.* **2014**, *15*, 3127; f) Y. J. Kang, J. Y. Lee, *Org. Electron.* **2016**, *32*, 109; g) L. Zhang, Y.-X. Zhang, Y. Hu, X.-B. Shi, Z.-Q. Jiang, Z.-K. Wang, L.-S. Liao, *ACS Appl. Mater. Interfaces* **2016**, *8*, 16186; h) J.-A. Seo, S. K. Jeon, M. S. Gong, J. Y. Lee, C. H. Noh, S. H. Kim, *J. Mater. Chem. C* **2015**, *3*, 4640; i) S. K. Jeon, J. Y. Lee, *Org. Electron.* **2015**, *27*, 202; j) N. Giebink, B. Dandrade, M. Weaver, J. Brown, S. Forrest, *J. Appl. Phys.* **2009**, *105*, 124514.

[4] a) S. Reineke, K. Walzer, K. Leo, *Phys. Rev. B* **2007**, *75*, 125328; b) C. Adachi, M. A. Baldo, S. R. Forrest, M. E. Thompson, *Appl. Phys. Lett.* **2000**, *77*, 904; c) Q. Wang, H. Aziz, *ACS Appl. Mater. Interfaces* **2013**, *5*, 8733; d) S. Kim, H. J. Bae, S. Park, W. Kim, J. Kim, J. S. Kim, Y. Jung, S. Sul, S.-G. Ihn, C. Noh, S. Kim, Y. You, *Nat. Commun.* **2018**, *9*, 1211; e) N. Giebink, B. D'Andrade, M. Weaver, P. Mackenzie, J. Brown, M. Thompson, S. Forrest, *J. Appl. Phys.* **2008**, *103*, 044509; f) N. K. Patel, S. Cina, J. H. Burroughes, *IEEE J. Sel. Top. Quantum Electron.* **2002**, *8*, 346.

[5] Y. Sun, N. C. Giebink, H. Kanno, B. Ma, M. E. Thompson, S. R. Forrest, *Nature* **2006**, *440*, 908.

[6] a) J. X. Sun, X. L. Zhu, H. J. Peng, M. Wong, H. S. Kwok, *Org. Electron.* **2007**, *8*, 305; b) N. Sun, Q. Wang, Y. Zhao, Y. Chen, D. Yang, F. Zhao, J. Chen, D. Ma, *Adv. Mater.* **2014**, *26*, 1617; c) Y. J. Cho, K. S. Yook, J. Y. Lee, *Sci. Rep.* **2015**, *5*, 7859; d) G. M. Farinola, R. Ragni, *Chem. Soc. Rev.* **2011**, *40*, 3467; e) G. M. Farinola, R. Ragni, *J. Solid*

**ADVANCED
SCIENCE NEWS**

www.advancedsciencenews.com

**ADVANCED
FUNCTIONAL
MATERIALS**

www.afm-journal.de

State Light. **2015**, *2*, 9; f) K. T. Kamtekar, A. P. Monkman, M. R. Bryce, *Adv. Mater.* **2010**, *22*, 572; g) M. Mazzeo, V. Vitale, F. Della Sala, M. Anni, G. Barbarella, L. Favaretto, G. Sotgiu, R. Cingolani, G. Gigli, *Adv. Mater.* **2005**, *17*, 34; h) J. Nishide, H. Nakanotani, Y. Hiraga, C. Adachi, *Appl. Phys. Lett.* **2014**, *104*, 233304; i) S. Reineke, F. Lindner, G. Schwartz, N. Seidler, K. Walzer, B. Lussem, K. Leo, *Nature* **2009**, *459*, 234; j) S. Reineke, M. Thomschke, B. Lüssem, K. Leo, *Rev. Mod. Phys.* **2013**, *85*, 1245.

[7] P. Peumans, A. Yakimov, S. R. Forrest, *J. Appl. Phys.* **2003**, *93*, 3693.

[8] a) A. Loudet, K. Burgess, *Chem. Rev.* **2007**, *107*, 4891; b) J. J. Chen, S. M. Conron, P. Erwin, M. Dimitriou, K. McAlahney, M. E. Thompson, *ACS Appl. Mater. Interfaces* **2015**, *7*, 662; c) M. Benstead, G. H. Mehl, R. W. Boyle, *Tetrahedron* **2011**, *67*, 3573; d) T. Bura, N. Leclerc, S. Fall, P. Lévêque, T. Heiser, P. Retailleau, S. Rihn, A. Mirloup, R. Ziessel, *J. Am. Chem. Soc.* **2012**, *134*, 17404; e) Y. Deng, Y.-y. Cheng, H. Liu, J. Mack, H. Lu, L.-g. Zhu, *Tetrahedron Lett.* **2014**, *55*, 3792; f) A. Kamkaew, S. H. Lim, H. B. Lee, L. V. Kiew, L. Y. Chung, K. Burgess, *Chem. Soc. Rev.* **2013**, *42*, 77; g) J. Karolin, L. B. A. Johansson, L. Strandberg, T. Ny, *J. Am. Chem. Soc.* **1994**, *116*, 7801; h) B. Kim, B. Ma, V. R. Donuru, H. Liu, J. M. J. Frechet, *Chem. Commun.* **2010**, *46*, 4148; i) S. Kolemen, O. A. Bozdemir, Y. Cakmak, G. Barin, S. Erten-Ela, M. Marszalek, J. H. Yum, S. M. Zakeeruddin, M. K. Nazeeruddin, M. Gratzel, E. U. Akkaya, *Chem. Sci.* **2011**, *2*, 949; j) T. Kowada, S. Yamaguchi, H. Fujinaga, K. Ohe, *Tetrahedron* **2011**, *67*, 3105; k) S. Kurata, T. Kanagawa, K. Yamada, M. Torimura, T. Yokomaku, Y. Kamagata, R. Kurane, *Nucleic Acids Res.* **2001**, *29*, 34e; l) M. R. Momeni, A. Brown, *J. Chem. Theory Comput.* **2015**, *11*, 2619; m) A. Orte, E. Debroye, M. J. Ruedas-Rama, E. Garcia-Fernandez, D. Robinson, L. Crovetto, E. M. Talavera, J. M. Alvarez-Pez, V. Leen, B. Verbelen, L. Cunha Dias de Rezende, W. Dehaen, J. Hofkens, M. Van der Auweraer, N. Boens, *RSC Adv.* **2016**, *6*, 102899; n) A. Schmitt, B. Hinkeldey, M. Wild, G. Jung, *J. Fluoresc.* **2009**, *19*, 755; o) A. Sutter, P. Retailleau, W.-C. Huang, H.-W. Lin, R. Ziessel, *New J. Chem.* **2014**, *38*, 1701; p) G. Ulrich, R. Ziessel, A. Harriman, *Angew. Chem., Int. Ed.* **2008**, *47*, 1184; q) X.-F. Zhang, J. Zhu, *J. Lumin.* **2019**, *212*, 286; r) J. Zhao, K. Xu, W. Yang, Z. Wang, F. Zhong, *Chem. Soc. Rev.* **2015**, *44*, 8904.

[9] a) J. Bañuelos, F. L. Arbeloa, V. Martinez, M. Liras, A. Costela, I. G. Moreno, I. L. Arbeloa, *Phys. Chem. Chem. Phys.* **2011**, *13*, 3437; b) J. H. Golden, J. W. Facendola, M. R. D. Sylvinson, C. Q. Baez, P. I. Djurovich, M. E. Thompson, *J. Org. Chem.* **2017**, *82*, 7215; c) J. H. Boyer, A. M. Haag, G. Sathyamoorthi, M.-L. Soong, K. Thangaraj, T. G. Pavlopoulos, *Heteroat. Chem.* **1993**, *4*, 39; d) G. Sathyamoorthi, M.-L. Soong, T. W. Ross, J. H. Boyer, *Heteroat. Chem.* **1993**, *4*, 603.

[10] Y. Kondo, K. Yoshiura, S. Kitera, H. Nishi, S. Oda, H. Gotoh, Y. Sasada, M. Yanai, T. Hatakeyama, *Nat. Photonics* **2019**, *13*, 678.

[11] J. F. Araneda, W. E. Piers, B. Heyne, M. Parvez, R. McDonald, *Angew. Chem., Int. Ed.* **2011**, *50*, 12214.

[12] a) L. Quan, Y. Chen, X. J. Lv, W. F. Fu, *Chem. - Eur. J.* **2012**, *18*, 14599; b) Y. Yang, X. Su, C. N. Carroll, I. Aprahamian, *Chem. Sci.* **2012**, *3*, 610.

[13] a) D. Wang, R. Liu, C. Chen, S. Wang, J. Chang, C. Wu, H. Zhu, E. R. Waclawik, *Dyes Pigm.* **2013**, *99*, 240; b) X. Zhu, H. Huang, R. Liu, X. Jin, Y. Li, D. Wang, Q. Wang, H. Zhu, *J. Mater. Chem. C* **2015**, *3*, 3774.

[14] M. E. Kondakova, J. C. Deaton, T. D. Pawlik, D. J. Giesen, D. Y. Kondakov, R. H. Young, T. L. Royster, D. L. Comfort, J. D. Shore, *J. Appl. Phys.* **2010**, *107*, 014515.

[15] a) Y. Kondo, K. Yoshiura, S. Kitera, H. Nishi, S. Oda, H. Gotoh, Y. Sasada, M. Yanai, T. Hatakeyama, *Nat. Photonics* **2019**, *13*, 678; b) S. Oda, B. Kawakami, R. Kawasumi, R. Okita, T. Hatakeyama, *Org. Lett.* **2019**, *21*, 9311.

[16] a) H. Ding, H. Yu, Y. Dong, R. Tian, G. Huang, D. A. Boothman, B. D. Sumer, J. Gao, *J. Controlled Release* **2011**, *156*, 276; b) M. H. W. Stopel, C. Blum, V. Subramaniam, *J. Phys. Chem. Lett.* **2014**, *5*, 3259; c) C. Sissa, A. Painelli, F. Terenziani, M. Trotta, R. Ragni, *Phys. Chem. Chem. Phys.* **2020**, *22*, 129.

[17] a) M. Y. Berezin, S. Achilefu, *Chem. Rev.* **2010**, *110*, 2641; b) O. Ostroverkhova, *Chem. Rev.* **2016**, *116*, 13279.

[18] A. Charaf-Eddin, B. Le Guennic, D. Jacquemin, *RSC Adv.* **2014**, *4*, 49449.

[19] S. Schols, A. Kadashchuk, P. Heremans, A. Helfer, U. Scherf, *Chemphyschem* **2009**, *10*, 1071.

[20] a) H. Nakanotani, K. Masui, J. Nishide, T. Shibata, C. Adachi, *Sci. Rep.* **2013**, *3*, 2127; b) Y. R. Cho, S. J. Cha, M. C. Suh, *Synth. Met.* **2015**, *209*, 47.

[21] a) X. H. Zhang, M. W. Liu, O. Y. Wong, C. S. Lee, H. L. Kwong, S. T. Lee, S. K. Wu, *Chem. Phys. Lett.* **2003**, *369*, 478; b) S. A. V. Slyke, C. H. Chen, C. W. Tang, *Appl. Phys. Lett.* **1996**, *69*, 2160; c) F. Guo, D. Ma, L. Wang, X. Jing, F. Wang, *Semicond. Sci. Technol.* **2005**, *20*, 310.

[22] M. Kumar, L. Pereira, *Nanomaterials* **2019**, *9*, 1307.

[23] S.-J. Su, H. Sasabe, T. Takeda, J. Kido, *Chem. Mater.* **2008**, *20*, 1691.

[24] a) S. A. Bagnich, S. Athanasopoulos, A. Rudnick, P. Schroegel, I. Bauer, N. C. Greenham, P. Strohriegl, A. Köhler, *J. Phys. Chem. C* **2015**, *119*, 2380; b) S. A. Bagnich, A. Rudnick, P. Schroegel, P. Strohriegl, A. Köhler, *Philos. Trans. R. Soc., A* **2015**, *373*, 20140446.

[25] H. Yoshida, K. Yoshizaki, *Org. Electron.* **2015**, *20*, 24.